

## Bottomonium from lattice QCD as a probe of the Quark-Gluon Plasma

This content has been downloaded from IOPscience. Please scroll down to see the full text.

2013 J. Phys.: Conf. Ser. 432 012014

(<http://iopscience.iop.org/1742-6596/432/1/012014>)

View [the table of contents for this issue](#), or go to the [journal homepage](#) for more

Download details:

IP Address: 149.157.1.188

This content was downloaded on 02/10/2013 at 17:25

Please note that [terms and conditions apply](#).

# Bottomonium from lattice QCD as a probe of the Quark-Gluon Plasma

**G. Aarts, C. Allton**

Department of Physics, Swansea University, Swansea, United Kingdom

**A. Kelly, J.-I. Skullerud**

Department of Mathematical Physics, National University of Ireland  
Maynooth, Maynooth, County Kildare, Ireland

**S. Kim**

Department of Physics, Sejong University, Seoul 143-747, Korea

**T. Harris, S. M. Ryan**

School of Mathematics, Trinity College, Dublin 2, Ireland

**M. P. Lombardo**

INFN-Laboratori Nazionali di Frascati, I-00044, Frascati (RM) Italy

**M. B. Oktay**

Physics Department, University of Utah, Salt Lake City, Utah, USA

**D. K. Sinclair**

HEP Division, Argonne National Laboratory, 9700 South Cass  
Avenue, Argonne, Illinois 60439, USA

**Abstract.** We study the temperature dependence of bottomonium for temperatures in the range  $0.4T_c < T < 2.1T_c$ , using non-relativistic dynamics for the bottom quark and full relativistic lattice QCD simulations for  $N_f = 2$  light flavors. We consider the behaviour of the correlators in Euclidean space, we analyze the associated spectral functions and we study the dependence on the momentum. Our results are amenable to a successful comparison with effective field theories. They help build a coherent picture of the behaviour of bottomonium in the plasma, consistent with the current LHC results.

## 1. Introduction

In this note we review the results on the spectrum of bottomonium in the quark-gluon plasma obtained by our FASTSUM collaboration [1–3] using a hybrid approach which combines exact relativistic dynamics for the light quarks with a non-relativistic approach for the bottom quark.

Recently, the first detailed results on the sequential Upsilon suppression in PbPb collision at LHC energies have appeared [4] (see also several talks at this meeting [5]). These results call for a quantitative understanding of the behaviour of bottomonium at high temperature. Due to their considerable experimental and theoretical interest these studies have been carried out in the past with a variety of techniques. We refer to recent excellent reviews [6, 7], as well as to our published papers, for background material and a complete set of references to early studies; here we limit ourselves to an exposition of our approach and results.

In the next Section we outline our approach to the problem. Next, we present the information we have obtained from the correlators alone. We continue by showing the results on the spectral functions. We finally discuss momentum dependence and we close with a short summary.

## 2. Five steps to Bottomonium

Our strategy is to treat as accurately as possible the light quarks, and use non-relativistic QCD (NRQCD) for the  $b$  quarks. In this way we hope to keep the systematic effects under control. Moreover, the accuracy of the results can be improved following the standard lattice techniques. In short outline, this is our ‘five steps approach to bottomonium’ strategy:

- i) Use full relativistic dynamics for up and down quarks (the inclusion of the strange quark is in progress). Gauge configurations with two degenerate dynamical light Wilson-type quark flavors are produced on highly anisotropic lattices, in a range of temperatures comprised between  $0.4T_c$  and  $2.1T_c$ . Details of the lattice action and parameters can be found in Refs. [8, 9].
- ii) We use NRQCD for the bottom quarks. Since NRQCD relies on the scale separation  $M \gg T$  and we study temperatures up to  $2T_c \simeq 400$  MeV, its application in our temperature range is fully justified. The light quarks, instead, feel the full relativistic dynamics. We computed NRQCD propagators on our configurations using a mean-field improved action with tree-level coefficients, which includes terms up to and including  $\mathcal{O}(v^4)$ , where  $v$  is the typical velocity of a bottom quark in bottomonium.
- iii) Analyze bottomonium correlators in Euclidean space. In standard conditions we expect an exponential decay. An analytic model for the Euclidean thermal behaviour is not known — we contented ourselves to study what to expect when quarks are no longer bound. Consider free quarks in continuum NRQCD with energy  $E_{\mathbf{p}} = \mathbf{p}^2/2M$ . The correlators for the  $S$  and  $P$  waves are

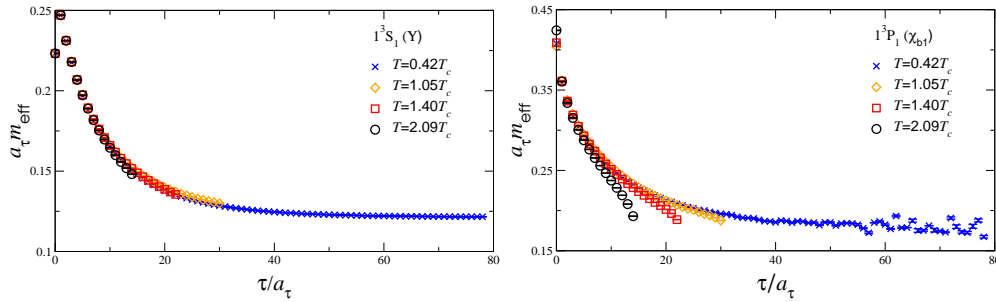


**Figure 1.** Effective mass plots for the  $\Upsilon$  (left) and  $\chi_{b1}$  (right) using point sources for various temperatures: note the different temperature dependence (Ref. [1]).

then of the form [12]

$$G_S(\tau) \sim \int \frac{d^3p}{(2\pi)^3} \exp(-2E_{\mathbf{p}}\tau) \sim \tau^{-3/2}, \quad (1)$$

$$G_P(\tau) \sim \int \frac{d^3p}{(2\pi)^3} \mathbf{p}^2 \exp(-2E_{\mathbf{p}}\tau) \sim \tau^{-5/2}, \quad (2)$$

i.e., they decay as a power for large euclidean time. Of course, interactions and finite lattice spacing and volume effects are expected to modify this in the realistic case. Moreover, again, this is a limiting high-temperature behaviour which should not be expected to hold even if the quarks unbind in the plasma. **iv)** Obtain spectral functions. In NRQCD, the spectral relation reduces to

$$G(\tau) = \int_{-2M}^{\infty} \frac{d\omega'}{\pi} \exp(-\omega'\tau) \rho(\omega') \quad (\text{NRQCD}), \quad (3)$$

even at nonzero temperature (note  $\omega = 2M + \omega'$ ). As a result, all problems associated with thermal boundary conditions are absent. We will extract NRQCD spectral functions from the euclidean correlators using the Maximum Entropy Method (MEM) [17].

**v)** Extract physics from the results, discuss phenomenology, validate effective models. We underscore that any meaningful comparison with experimental results and continuum physics requires control over systematic and lattice artifacts.

### 3. $\Upsilon$ and $\chi_b$ correlators in the plasma

We discuss here the results one can obtain from the analysis of correlators in Euclidean time, focusing on the  $\Upsilon$  and  $\chi_b$  states [1].

In Fig. 1, standard effective masses, defined by  $m_{\text{eff}}(\tau) = -\log[G(\tau)/G(\tau - a_\tau)]$ , are shown for both the  $\Upsilon$  and the  $\chi_{b1}$  propagators at various temperatures. Single exponential decay should yield a  $\tau$ -independent plateau. In both cases we find that at the lowest temperature,  $T = 0.42T_c$ , exponential behaviour is

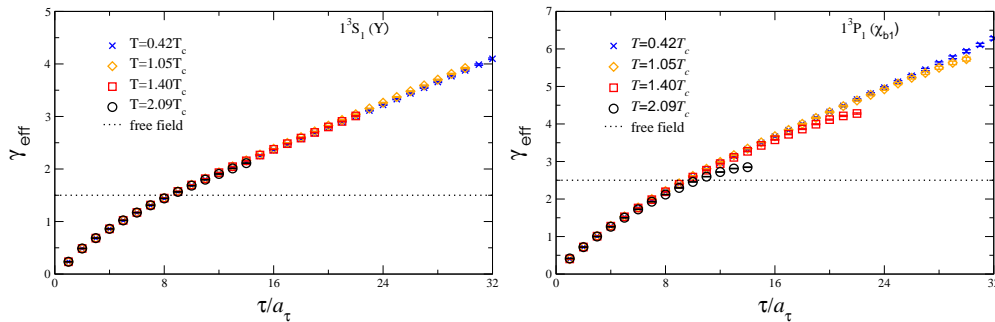


**Figure 2.** Effective exponents  $\gamma_{\text{eff}}(\tau)$  for the  $\Upsilon$  (left) and  $\chi_{b1}$  (right), as a function of Euclidean time for various temperatures. The dotted line indicates the non-interacting result in the continuum (Ref. [1]).

visible provided one goes to late euclidean times. At higher temperature we can see first indications that the  $\Upsilon$  is not sensitive to the quark-gluon plasma up to  $T \simeq 2T_c$ , while the  $\chi_b$  may melt at much lower temperatures, as exponential behaviour is no longer visible.

To visualize the approach to quasi-free behaviour we construct effective power plots [1], using the definition  $\gamma_{\text{eff}}(\tau) = -\tau \frac{G'(\tau)}{G(\tau)} = -\tau \frac{G(\tau+a_\tau) - G(\tau-a_\tau)}{2a_\tau G(\tau)}$ , where the prime denotes the (discretized) derivative. For a power decay,  $G(\tau) \sim \tau^{-\gamma}$ , this yields a constant result,  $\gamma_{\text{eff}}(\tau) = \gamma$ . The results are shown in Fig. 2. We confirm again that the  $\Upsilon$  displays a very mild temperature dependence, while for the  $\chi_{b1}$  the effective power tends to flatten out. As discussed, in the continuum limit and in the free case one should observe a flat behaviour. The observed flattening might thus suggest an approach to a free field behaviour, however several caveats apply. Also shown are the effective exponents in the continuum non-interacting limit. In the case of the  $\chi_{b1}$ , we observe that the effective exponent tends towards the non-interacting result at the highest temperature we consider.

To extend and validate these results, we proceed to the calculation of the spectral functions.

#### 4. Spectral functions

Our main results for the spectral functions [2] can be seen in Fig. 3, which shows that as the temperature is increased the ground state peaks of the  $\Upsilon$  and  $\eta_b$  remain visible. One caveat applies also here: the apparent width at zero temperature is most likely due to a lattice/MEM artifact, and this calls for an analysis of the discretization effects on the spectral function, which is one of our ongoing projects. The peaks associated to the excited states become suppressed at higher temperature and are no longer discernible at  $T/T_c \sim 1.68$ . The temperature dependence of the position and width of the ground state peaks is compared to analytical predictions obtained within the EFT formalism [18]. We note that the survival of the  $\Upsilon(1S)$  state and suppression of excited states is consistent with the recent experimental results [4].

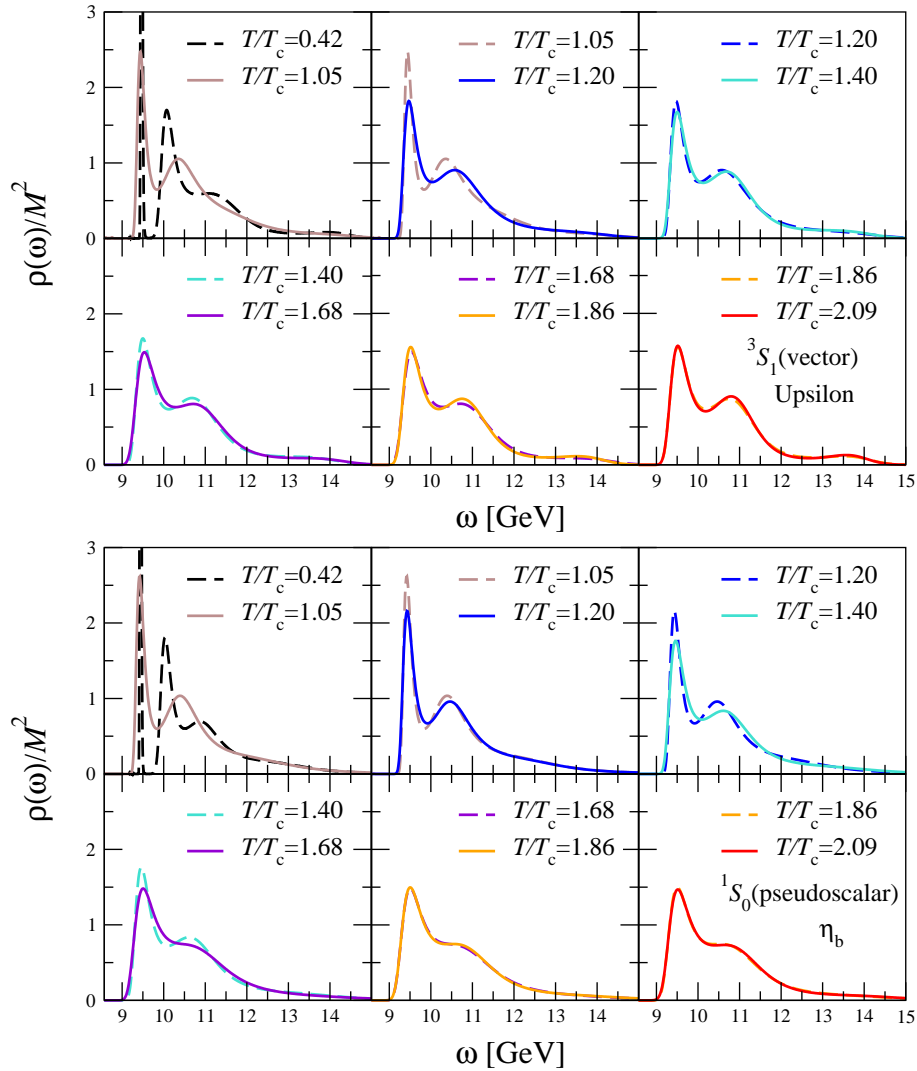


**Figure 3.** Spectral functions  $\rho(\omega)$ , normalised with the heavy quark mass, in the vector ( $\Upsilon$ ) channel (upper panel) and in the pseudoscalar ( $\eta_b$ ) channel (lower panel) for all temperature available. The subpanels are ordered from cold (top left) to hot (bottom right). Every subpanel contains two adjacent temperatures to facilitate the comparison (Ref. [2]).

From these spectral functions we can determine the mass (from the peak position) and (an upper bound on) the width of the ground state at each temperature. In Fig. 4 we show the temperature dependence of the mass shift  $\Delta E$ , normalised by the heavy quark mass and the temperature dependence of the width, normalised by the temperature.

We now contrast our results with analytic predictions derived assuming a weakly coupled plasma. According to Ref. [18], the thermal contribution to the

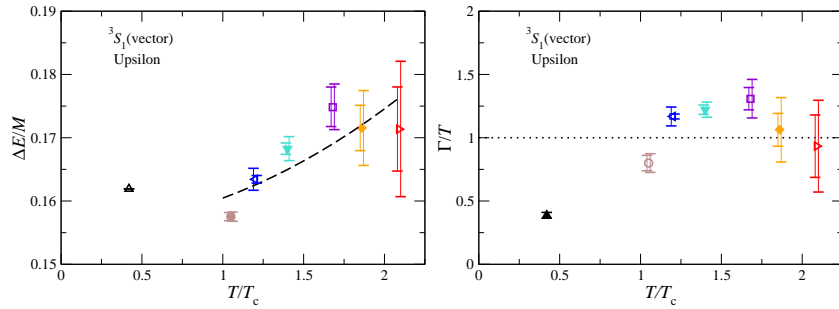


**Figure 4.** Position of the ground state peak  $\Delta E$ , normalised by the heavy quark mass (left), and the upper limit on the width of the ground state peak, normalised by the temperature (right), as a function of  $T/T_c$  in the vector ( $\Upsilon$ ) channel. Similar results have been obtained for the pseudoscalar ( $\eta_b$ ) channel (Ref. [2]).

width is given, at leading order in the weak coupling and large mass expansion, by

$$\frac{\Gamma}{T} = \frac{1156}{81} \alpha_s^3 \simeq 14.27 \alpha_s^3, \quad (4)$$

i.e., the width increases linearly with the temperature. If we take as an estimate from our results that  $\Gamma/T \sim 1$ , we find that this corresponds to  $\alpha_s \sim 0.4$ , which is a reasonable result. (It would be of interest to compute  $\alpha_s$  directly on our configurations.) In the same spirit the thermal mass shift is given in Ref. [18] by

$$\delta E_{\text{thermal}} = \frac{17\pi}{9} \alpha_s \frac{T^2}{M} \simeq 5.93 \alpha_s \frac{T^2}{M}. \quad (5)$$

In these simulations we have  $T_c \sim 220$  MeV,  $M \sim 5$  GeV. Taking these values together with  $\alpha_s \sim 0.4$  as determined above, Eq. (5) becomes

$$\frac{\delta E_{\text{thermal}}}{M} = 5.93 \alpha_s \left( \frac{T_c}{M} \right)^2 \left( \frac{T}{T_c} \right)^2 \sim 0.0046 \left( \frac{T}{T_c} \right)^2. \quad (6)$$

In order to contrast our results with this analytical prediction, we have compared the temperature dependence of the peak positions to the simple expression

$$\frac{\Delta E}{M} = c + 0.0046 \left( \frac{T}{T_c} \right)^2, \quad (7)$$

where  $c$  is a free parameter. This is shown by the dashed line in Fig. 4 (left panel). The numerical results and the analytic ones are not inconsistent, within the large errors, which encourages us to pursue further these studies.

## 5. Momentum Dependence

We extend now our study of bottomonium spectral functions in the quark-gluon plasma to nonzero momentum [3]. Note that effective theories analysis predict

| $\mathbf{n}$              | (1,0,0) | (1,1,0) | (1,1,1) | (2,0,0) | (2,1,0) | (2,1,1) | (2,2,0) |
|---------------------------|---------|---------|---------|---------|---------|---------|---------|
| $ \mathbf{p} $ (GeV)      | 0.634   | 0.900   | 1.10    | 1.23    | 1.38    | 1.52    | 1.73    |
| $v$ [ $\Upsilon(^3S_1)$ ] | 0.0670  | 0.0951  | 0.116   | 0.130   | 0.146   | 0.161   | 0.183   |
| $v$ [ $\eta_b(^1S_0)$ ]   | 0.0672  | 0.0954  | 0.117   | 0.130   | 0.146   | 0.161   | 0.183   |

**Table 1.** Nonzero momenta used in this study. Also indicated are the corresponding velocities  $v = |\mathbf{p}|/M_S$  of the ground states in the vector ( $\Upsilon$ ) and pseudoscalar ( $\eta_b$ ) channels, using the ground state masses determined previously [1],  $M_\Upsilon = 9.460$  GeV and  $M_{\eta_b} = 9.438$  GeV.

significant momentum effects at large momenta, and that current CMS results have been obtained at large momenta. So there is both phenomenological and experimental motivation for these studies.

The momenta and velocities that are accessible on the lattice are constrained by the discretization and the spatial lattice spacing. The lattice dispersion relation reads

$$a_s^2 \mathbf{p}^2 = 4 \sum_{i=1}^3 \sin^2 \frac{p_i}{2}, \quad p_i = \frac{2\pi n_i}{N_s}, \quad -\frac{N_s}{2} < n_i \leq \frac{N_s}{2}. \quad (8)$$

To avoid lattice artifacts, only momenta with  $n_i < N_s/4$  are used: we consider the combinations (and permutations thereof) given in table 1. The largest momentum, using  $\mathbf{n} = (2, 2, 0)$ , is  $|\mathbf{p}| \simeq 1.73$  GeV, corresponding to  $v = |\mathbf{p}|/M_S \simeq 0.2$ . Therefore, the range of velocities we consider is non-relativistic.

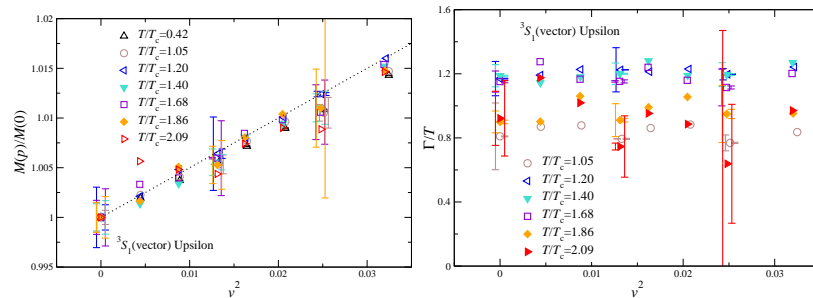


**Figure 5.** Position of the ground state peak  $M(\mathbf{p})/M(0)$  (left) and the upper limit on the width of the ground state peak, normalized by the temperature,  $\Gamma/T$  (right), as a function of the velocity squared ( $v^2$ ) in the vector ( $\Upsilon$ ) channel. Analogous results have been obtained for the the pseudoscalar ( $\eta_b$ ) channel. The dotted line in the left figure represents  $M(\mathbf{p})/M(0) = 1 + \frac{1}{2}v^2$  (Ref. [3]).

As in the zero momentum case, we extract masses and widths from our correlators using MEM, and we display them in Fig. 5. We observe that the



peak position increases linearly with  $v^2$ , as expected. Assuming the lowest-order, non-relativistic expression  $M(\mathbf{p}) = M(0) + \mathbf{p}^2/2M(0)$ , one finds

$$\frac{M(\mathbf{p})}{M(0)} = 1 + \frac{\mathbf{p}^2}{2M^2(0)} = 1 + \frac{1}{2}v^2, \quad (9)$$

which is indicated with the dotted lines in the left figures.

The dependence on the velocity can be compared with EFT predictions. In Ref. [19] a study of the velocity dependence was carried out in the context of QED, working in the rest frame of the bound state (i.e. the heat bath is moving). In order to compare with our setup, we consider the case in which the temperature is low enough for bound states to be present and that the velocities are non-relativistic. In that case, one finds [19], in the rest frame of the bound state and at leading order in the EFT expansion,

$$\frac{\Gamma_v}{\Gamma_0} = \frac{\sqrt{1-v^2}}{2v} \log\left(\frac{1+v}{1-v}\right), \quad (10)$$

where  $\Gamma_0$  is the width at rest. Interpreting the width as an inverse lifetime, one can express this result in the rest frame of the heat bath by dividing with the Lorentz factor  $\gamma = 1/\sqrt{1-v^2}$ . An expansion for non-relativistic velocities then yields

$$\frac{\Gamma_v}{\Gamma_0} = 1 - \frac{2v^2}{3} + \mathcal{O}(v^4). \quad (11)$$

If we apply this result to our study of bottomonium, we find that the effect of the nonzero velocity shows up as a correction at the percent level (recall that  $v^2 \lesssim 0.04$ ), which is beyond our level of precision but consistent with the observed  $v$  independence within errors. Similarly, additional thermal effects in the dispersion relation are currently beyond our level of precision. In summary, the observation in our low-momentum range are consistent with Ref. [19], and in order to observe the predicted non-trivial momentum dependence we need to explore larger momenta.

## 6. Summary

We have presented our results on bottomonium in the quark-gluon plasma, for temperatures up to  $2.1T_c$ , at the threshold of the region currently explored by LHC heavy-ions experiments. Our analysis uses full relativistic gauge field configurations, and a non-relativistic approach for the bottom quarks. Our goal is to reach a quantitative, systematic control on the results, which is called for by the new level of experimental accuracy. Related to this, we aim at understanding in detail the range of validity of the available effective models. This is a task of foremost importance, since an accurate analytic modeling is needed as an input to real time evolution.

Our results so far were based on a set of gauge field configurations obtained with two flavors of dynamical quarks. We have used anisotropic lattices in order to maximize the number of points in Euclidean time — a much needed feature for a successful MEM analysis. In this way even on our hottest lattices

( $T = 2.1T_c$ ) we have been able to analyze correlators and proceed to the calculation of the spectral functions.

On these lattice ensembles we have observed that the temperature affects only very mildly the  $\Upsilon$  and  $\eta_b$  correlators, suggesting the survival of the fundamental states in these channels up to  $T \simeq 2T_c$ . A subsequent calculation of the spectral functions carried out with a MEM analysis has confirmed the survival of the fundamental states and revealed the melting of the excited states in the same channels above  $1.4T_c$ . The correlators for the  $\chi_b$  and  $h_b$  indicate a quick melting of these states above  $T_c$ .

On the methodological side, we have argued that the peculiar nature of non-relativistic dynamics greatly simplifies the MEM analysis and enhances its reliability. We have invested a considerable effort in monitoring the systematic effects associated with the MEM analysis, which is described in our papers, and we feel that we have them well under control. The special form of the NRQCD spectral relations shows that the NRQCD spectral function is an inverse Laplace transform of the correlator. In a nutshell, this makes the MEM analysis easier than in the full relativistic case, and perhaps opens the way to a direct, more simple evaluation of the spectral functions themselves.

Our activities in the near future are evolving along different lines. Firstly, new results which will be available in the near future include a MEM analysis for the  $\chi_b$  and  $h_b$  channels.

Secondly, we wish to approach more closely the continuum limit, with a physical matter content. To this end, simulations with a reduced lattice spacing, and the inclusion of the strange quarks, are already in progress. On the NRQCD side, on the new  $N_f = 2 + 1$  lattices the quark mass is tuned precisely using the kinetic mass and the lattice NRQCD dispersion relation. Moreover we are considering using the 1-loop determinations of the  $\sigma \cdot B$  term in the NRQCD coefficients which has recently produced an impressive improvement in the determination of the (zero temperature) hyperfine splitting [20]. All this will enhance the control over various lattice systematic errors. In a longer term perspective, relativistic beauty might also become feasible on these finer lattices, mirroring the approach that is already being followed for charmonium [8, 21]. This will provide a definitive check of the NRQCD approach.

Next, as for the momentum dependence, we have mentioned that both experimental and phenomenological activities call for calculations at larger momenta: a sizable dependence is expected at large momenta and large momenta are those studied by CMS. Large momentum studies will be possible on our finer lattices and this is being planned.

As a final remark, leading to further developments, an important aspect of our study is the comparison with effective theories. Within our limited precision, and limited explored range, the comparison has been satisfactory. This motivates us to enhance this analysis in the future. To carry out this program, besides the improvement already described, we will have to explore a wider set of parameters. One economic way of doing this is to vary the heavy quark mass, studying artificial mesons: this has been very helpful at zero temperature in cross checking lattice results and effective model predictions — for instance the results for the light meson spectrum are being compared with

chiral perturbation theory and the heavy meson spectrum with heavy quark effective theory. In the same spirit we would like to know the dependence of the bottomonium spectrum on the heavy quark mass, and temperature, and compare it with various effective models in their respective ranges of applicability. Remember in fact that different effective models hold true in correspondence with different relative values of the relevant scales such as  $M, M\alpha_s, T, M\alpha_s^2, m_D$ , so upon varying mass and temperatures one should observe a crossover between different behaviours, thus building confidence in using the corresponding models. This program has started and its first, preliminary results have been reported at Lattice 2012 [22].

### Acknowledgments

We wish to thank the Organisers for their suggestion that MPL replace the intended invited speaker — S.M. Ryan — who had to cancel her participation, so that our work could still be presented at the meeting.

### References

- [1] G. Aarts, S. Kim, M. P. Lombardo, M. B. Oktay, S. M. Ryan, D. K. Sinclair, J. -I. Skullerud, Phys. Rev. Lett. **106** (2011) 061602
- [2] G. Aarts, C. Allton, S. Kim, M. P. Lombardo, M. B. Oktay, S. M. Ryan, D. K. Sinclair and J. I. Skullerud, JHEP **1111** (2011) 103
- [3] G. Aarts, C. Allton, S. Kim, M. P. Lombardo, M. B. Oktay, S. M. Ryan, D. K. Sinclair and J. -I. Skullerud, arXiv:1210.2903 [hep-lat].
- [4] S. Chatrchyan *et al.* [CMS Collaboration], arXiv:1208.2826 [nucl-ex].
- [5] G. Breto-Rangel, P. Braun-Munzinger, Nu Xu, M. Strickland, P. Petreczki, this Volume
- [6] T. Hatsuda, Review talk at *Quark Matter 2012*, to appear in the Proceedings
- [7] O. Kaczmarek, Review talk at *Hard Probes 2012*, arXiv:1208.4075 [hep-lat].
- [8] G. Aarts, C. Allton, M. B. Oktay, M. Peardon and J. I. Skullerud, Phys. Rev. D **76** (2007) 094513
- [9] R. Morrin, A. Ó Cais, M. Peardon, S. M. Ryan and J. I. Skullerud, Phys. Rev. D **74** (2006) 014505
- [10] M. Laine, O. Philipsen, P. Romatschke and M. Tassler, JHEP **0703** (2007) 054
- [11] M. Laine, JHEP **0705** (2007) 028
- [12] Y. Burnier, M. Laine and M. Vepsäläinen, JHEP **0801** (2008) 043
- [13] N. Brambilla, J. Ghiglieri, A. Vairo and P. Petreczky, Phys. Rev. D **78** (2008) 014017
- [14] N. Brambilla, M. A. Escobedo, J. Ghiglieri and A. Vairo, JHEP **1112** (2011) 116
- [15] A. Beraudo, J. P. Blaizot and C. Ratti, Nucl. Phys. A **806** (2008) 312
- [16] A. Beraudo, J. P. Blaizot, P. Faccioli and G. Garberoglio, Nucl. Phys. A **846** (2010) 104
- [17] M. Asakawa, T. Hatsuda, Y. Nakahara, Prog. Part. Nucl. Phys. **46** (2001) 459-508
- [18] N. Brambilla, M. A. Escobedo, J. Ghiglieri, J. Soto, A. Vairo, JHEP **1009** (2010) 038
- [19] M. A. Escobedo, J. Soto and M. Mannarelli, Phys. Rev. D **84** (2011) 016008
- [20] T. C. Hammant, A. G. Hart, G. M. von Hippel, R. R. Horgan and C. J. Monahan, Phys. Rev. Lett. **107**, 112002 (2011)
- [21] A. Kelly, D. B. Mehta, M. B. Oktay, J.-I. Skullerud, *Charm diffusion from 2-flavor lattice QCD*, in preparation; A. Kelly, *Spectral functions of charmonium in 2+1 flavour lattice QCD*, poster at Strong and Electroweak Matter 2012.
- [22] S. Kim, G. Aarts, C. Allton, M. P. Lombardo, M. B. Oktay, S. M. Ryan, D. K. Sinclair and J. -I. Skullerud, arXiv:1210.7586 [hep-lat].